

Investigation of soot sediments in particulate filters and engine components

I. Manke^{1,2}, M. Strobl³, N. Kardjilov², A. Hilger², W. Treimer⁴, M. Dawson², J. Banhart^{1,2}

¹*Institute of Materials Science and Technology, Technische Universität Berlin, Hardenbergstr. 36, 10623 Berlin, Germany,* ²*Helmholtz Centre Berlin, Glienicker Str. 100, 14109 Berlin, Germany,* ³*University of Heidelberg, Im Neuenheimer Feld 253, 69120 Heidelberg, Germany,* ⁴*University of Applied Sciences (TFH) Berlin, Luxemburger Str. 10, 13353 Berlin, Germany*

Abstract

The investigation of soot sediments can be crucial for the development of improved components for combustion engines and for the identification of potential hazards. Here we present a number of exemplary studies of soot sediments in such components, which demonstrate the potential of neutron tomography in this field. Neutrons are well suited for imaging massive metal parts, which they can penetrate easily, allowing for imaging entire components with volumes of tens to hundreds of cubic centimeters non-destructively, whilst still being sensitive to lighter elements; in this case hydrogen-containing soot. Up-to-date techniques such as high-resolution and monochromatic neutron tomography have been applied in order to investigate soot sediments from fine particles in the pores of SiC diesel soot filters to massive structures in vent tubes of an aircraft.

Key words: neutron imaging, tomography, particulate filters, soot sediments, industrial applications

Introduction

Any engine that is operated by burning hydrocarbons produces soot. The soot consequently contaminates all engine components involved in the handling of exhaust gases. Thereby soot sediments may accumulate in different parts of an engine either accidentally or intentionally e.g. in a soot filter [1]. In the first case, sediments can cause disturbances in the gas flow which can lead to malfunctions or, in extreme cases, to severe damage and even the destruction of the engine. Hence, the investigation of sediments is of particular interest to the automotive and aircraft industry. On the other hand diesel particulate filters recently gained importance because of environmental and health considerations. Consequently, soot filters have become a focus of political and industrial interest. Modern vehicles have to comply with high standards and strict regulations concerning pollution and the protection of the environment. Although effective filters have been developed and are now available,

drawbacks such as residual soot in the fine capillaries of SiC filters still constitute major problems in the development and optimization of an improved second generation of these devices.

In instances where there is no or only limited access to the area of soot contamination, the application of a tomographic technique is required since the brittle nature of the sediments prevents the use of invasive techniques [2,3]. For locating and analyzing the soot sediments in often massive metal engine components that are not easily penetrated by X-rays, neutrons are the best choice. In contrast to X-rays, neutrons can penetrate thick layers of metal and are still sensitive to even small sediments of soot, depending on their hydrogen content [3, 4]. This is due to the fact that neutrons, unlike X-rays, do not interact with the electrical charge of the electrons within atoms, but with the atomic nuclei. As a result, there is no direct dependence between attenuation and atomic number - hydrogen, for example, strongly attenuates a neutron beam, while steel or aluminum layers of the order of centimeters can be penetrated [3]. This makes neutron imaging especially suitable to investigate metallic engineering components. In industrial research the high attenuation coefficient of hydrogen for neutrons is exploited to visualize hydrogen and hydrogen containing materials, such as water in fuel cells [5-11], hydrogen in batteries [12], hydrogen storage materials [13] and oil in engines [14]. Several previous investigations of soot-contaminated tubes and particulate filters have been reported [15-17]. Furthermore, Lehmann et al. have performed similar investigations at the Paul Scherrer Institute (PSI) [18]. However, the low number of publications in contrast to the high potential of the technique in this field might be attributed to the fact that such investigations are mostly initiated by industry.

Here, we present an overview of recent applications of neutron imaging on soot contaminations in different engineering components including related methodical and technical developments at the neutron imaging facility at the Hahn-Meitner research reactor of the Helmholtz Centre Berlin.

Experimental Setup

Tomographic investigations with polychromatic neutrons were performed at the neutron tomography instrument CONRAD/V7 at the Helmholtz Centre Berlin [16]. It is located in the neutron guide hall at the Hahn-Meitner research reactor where low-energy (cold) neutrons are used for experimental purposes. The transmitted beam is detected by a position sensitive detector behind the sample (Fig. 1). The main part of the detector system is the 16-bit low-noise CCD camera (Andor DW436N with 2048×2048 pixel) which is focused on a neutron-

sensitive scintillator screen by a lens system. Experiments with monochromatic neutrons have also been performed at the V-12 instrument position [17]. An asymmetric perfect Si crystal monochromator in the beam of the cold neutron guide NL4 provided a highly monochromatic beam with a wavelength of 0.45 nm ($\Delta\lambda/\lambda \cong 2\%$). This led to a low flux density of approximately $5 \times 10^3 \text{ n cm}^{-2}\text{s}^{-1}$. The L/D ratio could be determined by measuring the line spread of a Gd edge to be $\cong 170$ in the horizontal direction and $\cong 110$ in the vertical direction. The limitations imposed by both the detector system and the beam collimation resulted in a horizontal/vertical spatial resolution of 300 $\mu\text{m}/400 \mu\text{m}$ at a sample to detector distance of 5 cm. Further details can be found in the literature [17].

Experimental results

The first example to be presented is an investigation of steel tubes that transport hot exhaust gases away from an aircraft engine (Fig. 2). The vent pipes had an inner and outer diameter of about 2.0 cm and 2.4 cm, respectively. In some of the tubes such a large quantity of fuel and oil sediments had been deposited that the gas stream was seriously hindered; blockage could cause serious damage to the engine. Previous X-ray investigations had failed to reveal the deposited materials and cutting the tube would have destroyed the brittle sediments. Therefore, neutron tomography was employed in order to examine the sediments in the vent pipes. A monochromatic beam was used in order to allow the energy-dependent attenuation coefficient of the materials within the sample to be determined more accurately. The result in Fig. 2b clearly revealed the eligibility of neutron tomography in general. Soot sediments and sediment particles could easily be visualized and quantified with the resolution of the instrument (see above). The lower flux of the monochromatic beam had to be compensated by significantly increased exposure times. While a tomogram could be recorded in typically 2-3 h in the conventional setup, it took about 12-36 h with monochromatic neutrons. However, this was justified by the ability to separate (from their differing attenuation coefficients) the different layers of the fuel sediments by their hydrogen content (Fig. 3). Older sediments contained less hydrogen because they had been exposed to high temperatures and the gas flow for a longer time than more recent sediments. This is obvious for the simple case of sediments along the walls, where lower layers are older than upper layers. Hence, these attenuation differences provide information about the history of sedimentation of the residues, which can help in understanding the reasons of increased sedimentation in some cases.

Monochromatic neutrons can increase the sensitivity to hydrogen variations. However, in the case of strong variations in the distribution of hydrogen content, even polychromatic neutrons can be used to obtain quantitative results. In the next example, an investigation of soot sediments in a part of a combustion chamber of an engine is shown. The massive component has a diameter of about 12 cm and a height of a few cm. Neutron tomography was performed, based on 600 radiographic projection images over a range of 180° that were recorded in a total exposure time of about 10 h. The achieved spatial resolution was approximately 200 μm. Figure 4 displays the corresponding tomographic reconstruction, which is colored in order to visualize the detected soot contaminations. A corresponding histogram is shown in Fig. 5. The soot sediment distribution in the inner part of the gas flow channels of the component are of major interest for the investigation. As in the cross section through the tomogram in Fig. 2, large soot agglomerations can be identified. In this region contaminations with soot sediments are especially problematic because they strongly hinder gas flow and might cause a malfunction of the component and consequently also of the engine. Some contaminated locations are marked with numbers that can be assigned to different hydrogen contents or densities of the residues (see Fig. 4).

A more complex situation is found in particulate filters or similar components. The soot contaminations that are of interest are not only located in the hollow spaces, but are also spread along the surface of the walls of the filters. The soot forms a rather thin layer, typically between a few 10 μm and a few 100 μm thick, and even extends into the porous surface where it can be found within the walls. In addition, the hydrogen content of the sediments in modern filters is very low, yielding a very low attenuation that is comparable to that of the surrounding SiC.

Two different materials are mainly used for particulate filters: steel and SiC. Fig. 6 shows a part of a tomogram of a steel filter. For the tomogram, 600 projections were recorded with 5 min. exposure time each. Due to the large size of the object and high attenuation of steel a polychromatic beam had to be used in order to achieve reasonable transmission and moderate exposure times. Although it might be possible to identify some sediments, this investigation is clearly close to the limit of what the method can provide.

A part of a tomogram of a SiC filter taken under similar measurement conditions is shown in Fig. 7a. Here, the separation of soot sediments (attempt to color them green) and the SiC matrix failed due to limited spatial resolution. Consequently, a new trial was undertaken with a new detector set-up.

In Fig. 7b a comparable part of the same filter is shown from a second measurement. Due to the new set-up employing improved optics and a new scintillator the achieved spatial resolution could be increased from the initial 200 μm (left image) to about 70 μm . This time the resolution was clearly sufficient to separate SiC parts with significant soot contamination (soot contaminated areas are colored red). In Fig. 7c a cross section along the gas flow channels is shown for comparison. The non-uniform distribution of the soot-contaminated areas provides important information for further filter design and development.

Conclusions

We have shown that neutron tomography is well suited to detecting soot contaminations and other fuel and lubricate residues inside different types of engineering and industrial components. When the contaminations are located in initially hollow spaces visualization is possible even in the presence of (comparably) strongly attenuating materials such as iron. The hydrogen distribution inside fuel residues, for example, reveals information about how these sediments develop. It can be concluded that neutron tomography is not limited to simple components such as tubes, but can be applied even to complicated and massive engineering components.

In contrast, very thin soot layers in diesel particulate filters are very difficult to detect. In modern filters the residues are burned at high temperatures, which reduces the hydrogen content of the soot dramatically. The attenuation of almost pure carbon is very low. Therefore, layers of carbon with a thickness very close to the spatial resolution of a typical neutron imaging instrument are still difficult to image, especially when they are located at the walls of steel.

In SiC filters the situation is different. Although carbon sediments are hard to detect because the attenuation coefficients of SiC and pure or slightly hydrogen-contaminated carbon are very similar, with the new high resolution setups available today the situation has improved significantly. The achievable spatial resolution below 100 μm allows the detection of soot that is located in the small pores of the SiC walls. In difficult cases, a comparison of clean and contaminated filters can provide increased reliability.

In future, a combination of high resolution set-ups and monochromatic neutron imaging might help to improve image quality and information content also for particulate filters. This would

allow the elimination of beam hardening effects and more precise quantitative reconstructions of attenuation coefficients.

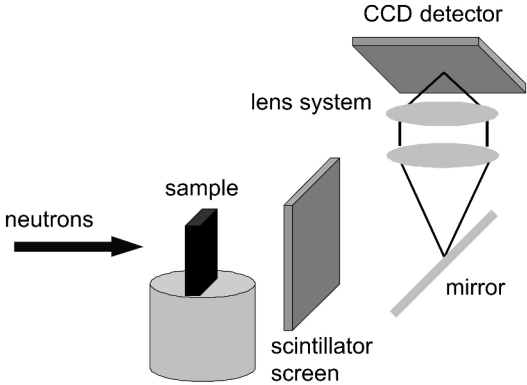


Fig. 1: Schematic drawing of the experimental set-up

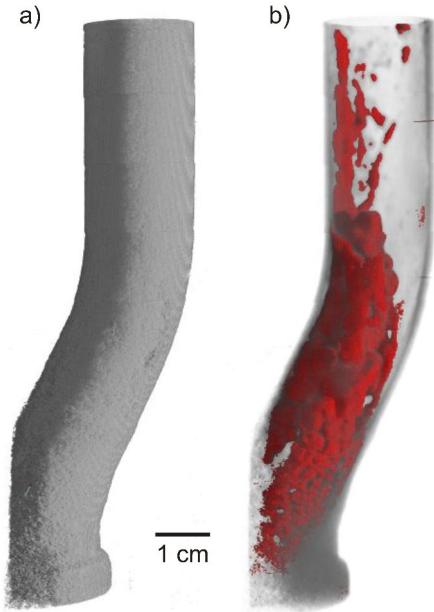


Fig.2: Soot in a pipe: neutron tomogram of a steel pipe with a diameter of 2 cm. a) external view, b) the metal was made transparent and the image reveals the soot distribution inside of the pipe (red).

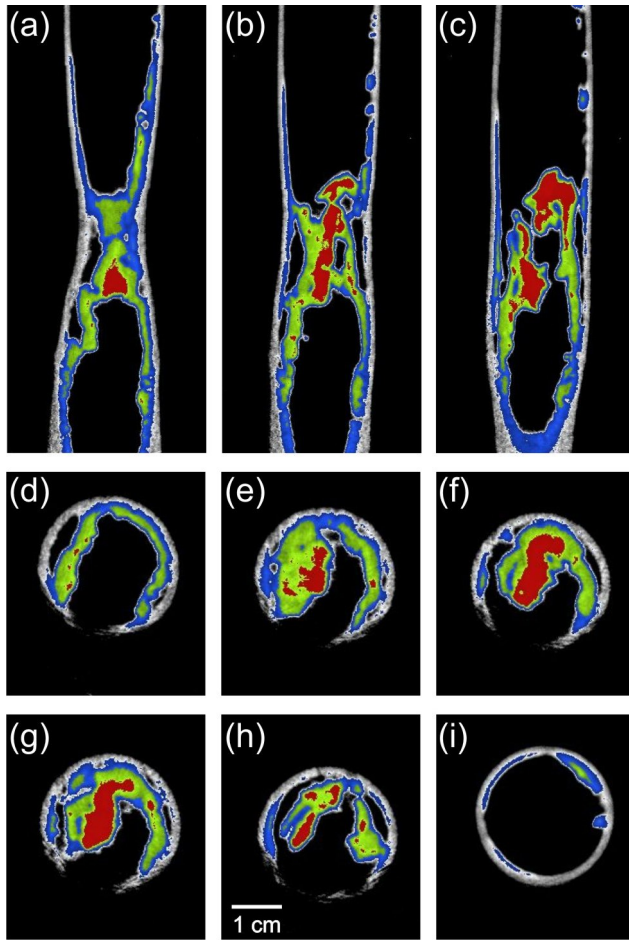


Fig. 3: Soot distribution inside the steel pipe shown in Fig. 1. The uppermost three images are different cross sections along the long axis. The six images below are horizontal cross sections through the pipe. Red parts correspond to high attenuation coefficients, green and blue to lower ones. Variations in the attenuation coefficient are caused by different hydrogen contents of the soot.

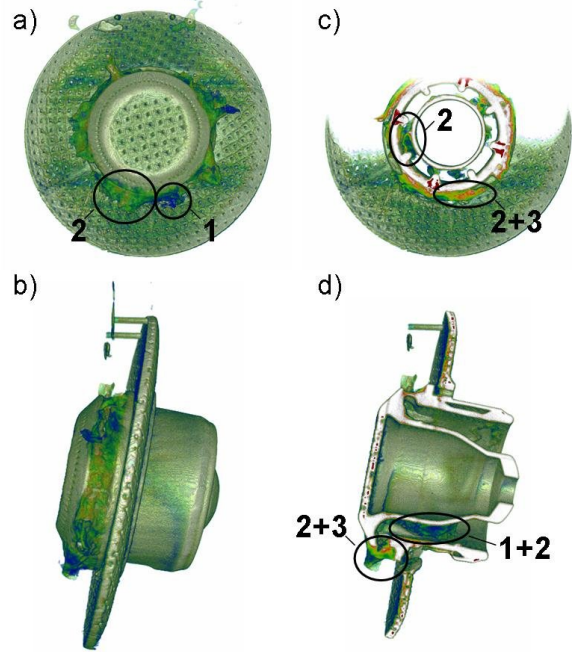


Fig. 4: Neutron tomographic image of a combustion chamber. Colored areas mark the locations of fuel and lubricate residues. The varying attenuation coefficient is mainly a result of the different hydrogen contents in the material. The histogram applied for his image is shown in Fig. 5. The numbers mark areas with specific attenuation coefficients (see Fig. 5). a) front view, b) side view, c) cross section through the plane and d) vertical cross section.

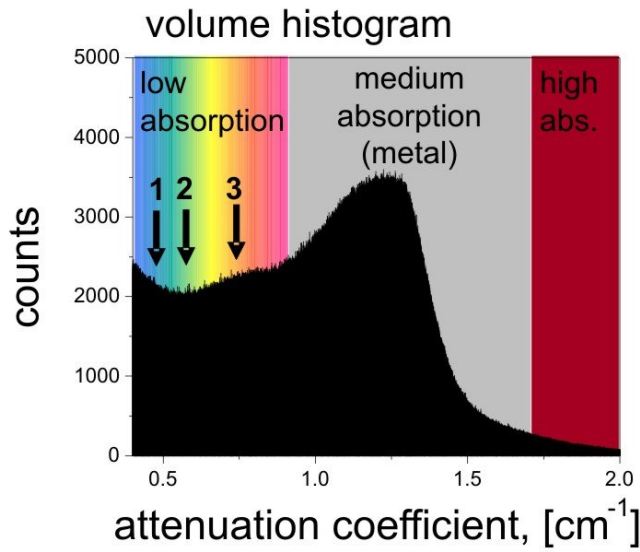


Fig. 5 Histogram settings used to display the hydrogen contents of fuel and lubricate residues in Fig. 4. Three points that can be assigned to locations in the sample are marked by arrows (see also Fig. 4)

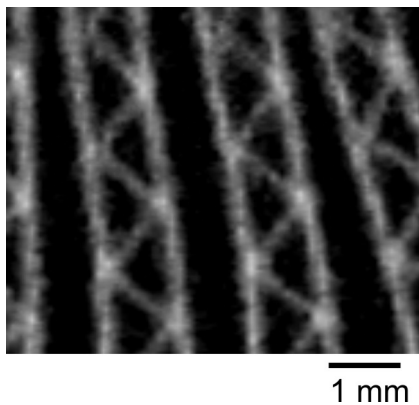


Fig. 6: Part of the tomogram of a particulate filter made of steel. The rather low hydrogen content of the soot yields a very low attenuation coefficient. In the high attenuating steel the soot is practically invisible.

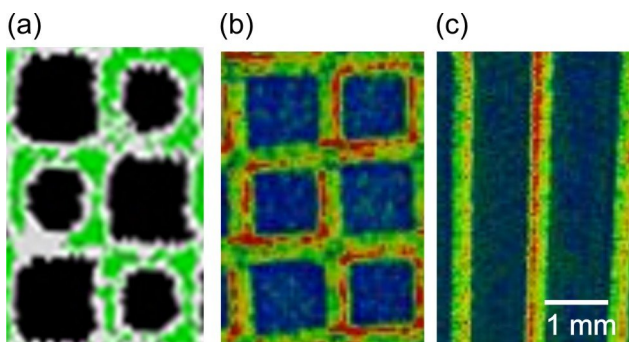


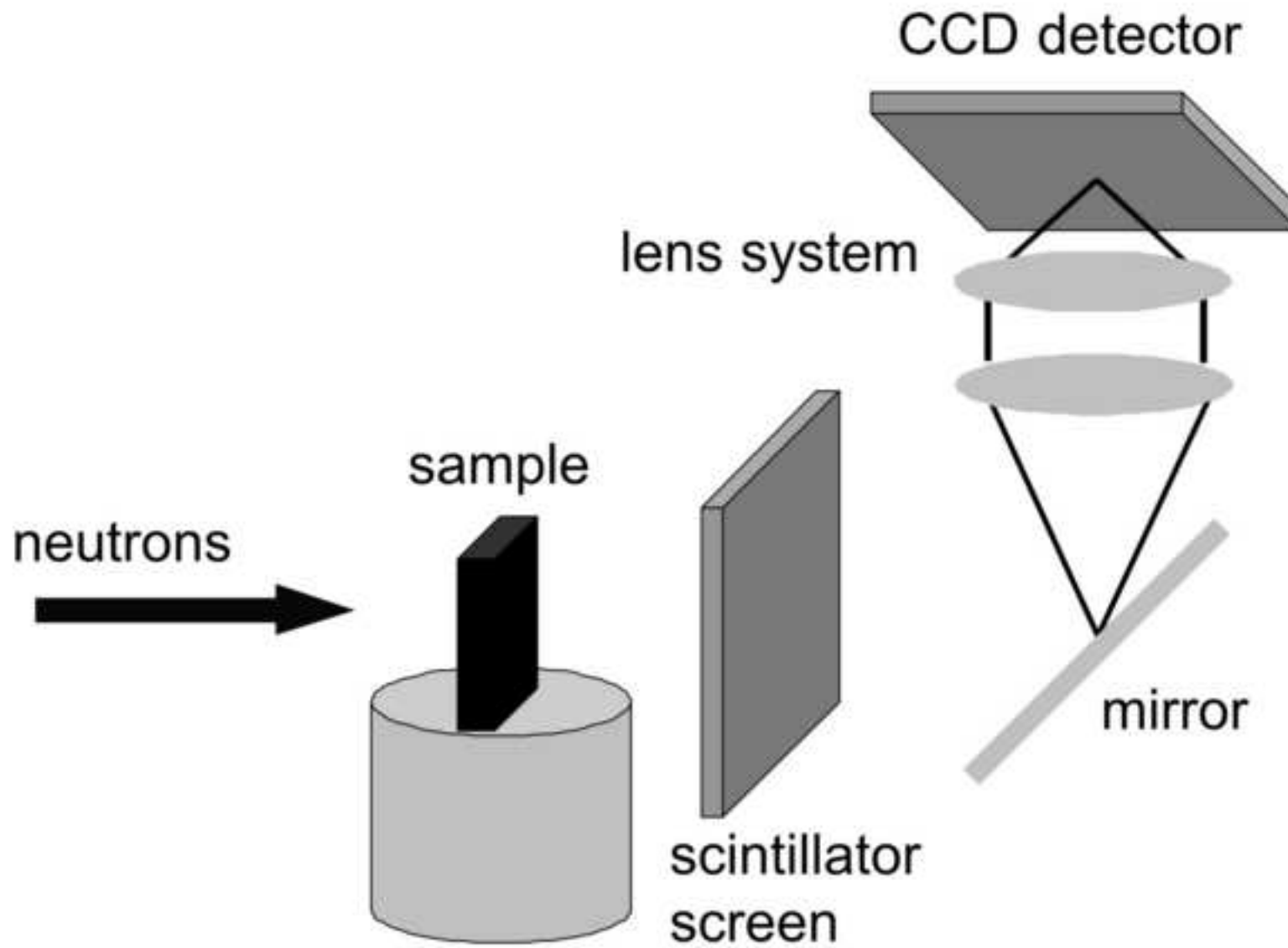
Fig. 7: Cross sections through different neutron tomograms of a SiC-particulate filter. The left image shows a vertical cross section through the gas channel obtained with a standard imaging setup that does not allow detection of the soot located mainly within the SiC walls. The image in the center shows a region of the same filter imaged with a high resolution set-up. Here, the soot in the walls can be visualized very clearly (marked in red). Right: Cross section along the gas channels of the high resolution tomogram.

References

- [1] M. Matti Maricq, *Journal of Aerosol Science Review* 38 (2007), p 1079
- [2] A.C. Kak, M. Slaney, *Principals of Computerized Tomographic Imaging*, IEEE Press, NewYork, 1987
- [3] E. Lehmann, N. Kardjilov, in J. Banhart (Ed.): *Advanced Tomographic Methods in Materials Research and Engineering*, Oxford University Press (2008)
- [4] B. Schillinger, E. Lehmann., P. Vontobel, *Physica B* 59 (2000), 276
- [5] R. Satija, D.L. Jacobson, M. Arif, S.A. Werner, *J. Power Sources* 129 (2004) 238
- [6] J. Zhang, D.Kramer, R. Shimoj, Y. Ono, E. Lehmann, A. Wokaun, K. Shinohara, G.G. Scherer, *Electrochimica Acta* 51 (2006) 2715
- [7] I. Manke, Ch. Hartnig, N. Kardjilov, M. Messerschmidt, A. Hilger, M. Strobl, W. Lehnert, J. Banhart, *Appl. Phys. Lett.* 92 (2008) 244101
- [8] Ch. Hartnig, I. Manke, N. Kardjilov, A. Hilger, M. Grünerbel, J. Kaczerowski, J. Banhart, W. Lehnert, *J. Power Sources* 176 (2008) 452
- [9] I. Manke, Ch. Hartnig, M. Grünerbel, J. Kaczerowski, W. Lehnert, N. Kardjilov, A. Hilger, W. Treimer, M. Strobl J. Banhart, *Appl. Phys. Lett.* 90, (2007) 184101
- [10] M. A. Hickner, N. P. Siegel, K. S. Chen, D. S. Hussey D. L. Jacobson and M. Arif, *J. Electrochem. Soc.*, 155, 427 (2008)
- [11] P. Boillat, D. Kramer, B.C. Seyfang, G. Frei, E. Lehmann, G.G. Scherer, A. Wokaun, Y. Ichikawa, Y. Tasaki and K. Shinohara, *Electrochem. Commun.* 10 (2008) 546

- [12] I. Manke, J. Banhart, A. Haibel, A. Rack, S. Zabler, N. Kardjilov, A. Hilger, A. Melzer, H. Riesemeier, Appl. Phys. Lett. 90 (2007) 214102
- [13] H. Sakaguchia, Y. Satakea, K. Hatakeyamaa, S. Fujineb, K. Yonedab, M. Matsubayashic, T. Esakaa, Journal of Alloys and Compounds 354 (2003) 208
- [14] B. Schillinger, J. Brunner, E. Calzada, Physica B: Condensed Matter 385, (2006) 921
- [15] B. Ismail, D. Ewing^a, J.-S. Chang and J. S. Cotton, Journal of Aerosol Science 35 (2004), 1275
- [16] N. Kardjilov, A. Hilger, I. Manke, M. Strobl, b, W. Treimer and J. Banhart, Nucl. Instr. and Meth. A, 542 (2005) 16
- [17] M. Strobl, W. Treimer, C. Ritzoulis, A. G. Wagh, S. Abbas and I. Manke, J. Appl. Cryst. 40 (2007) 463
- [18] E. Lehmann, private communication
- [19] For further information see: <http://www.volumegraphics.com/>

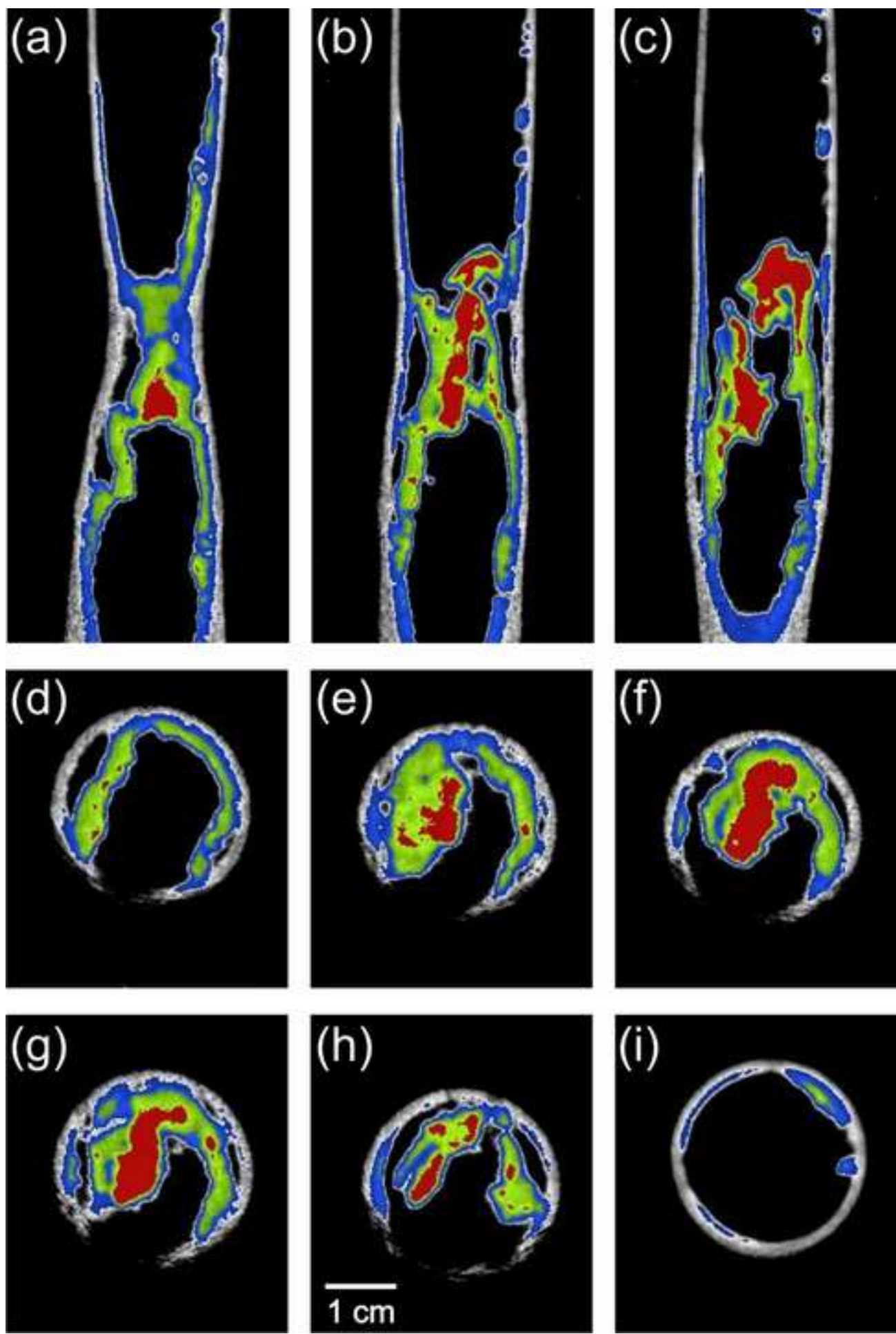
Figure(s)
[Click here to download high resolution image](#)

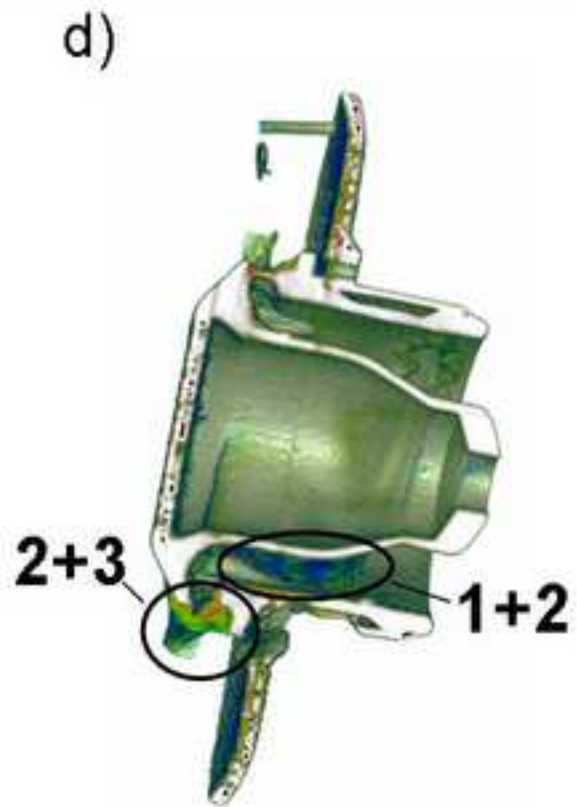
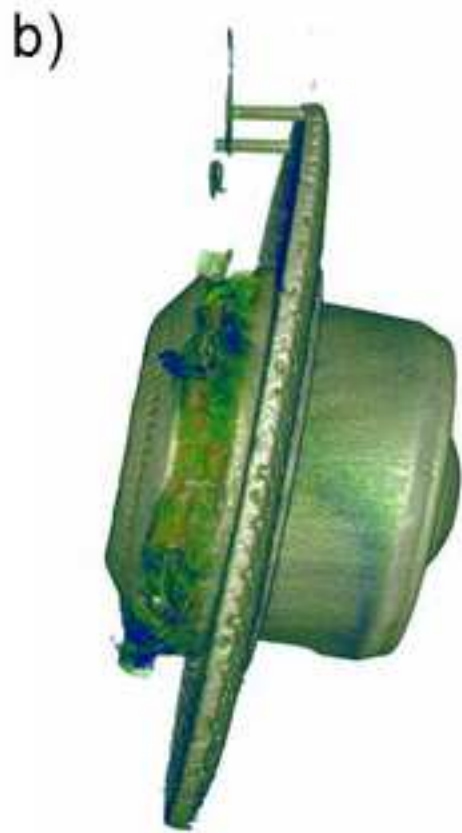
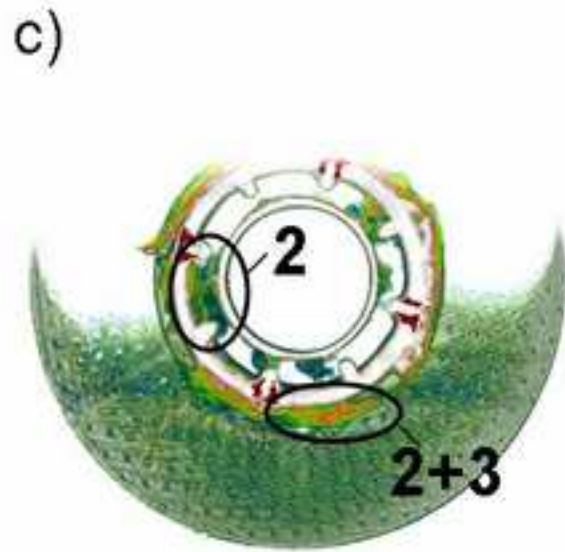
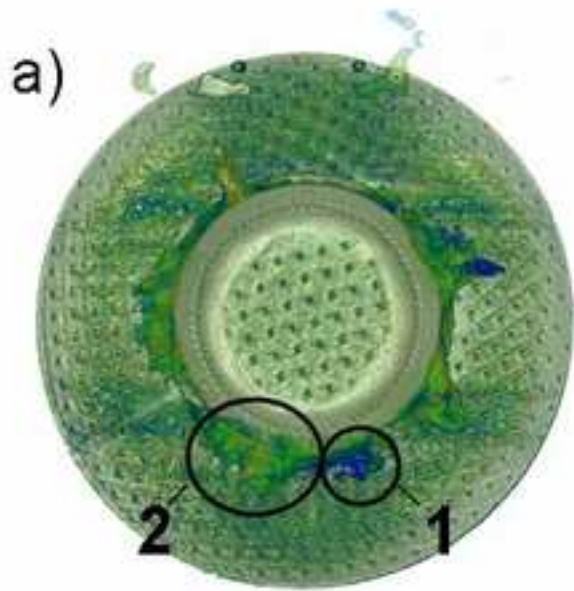


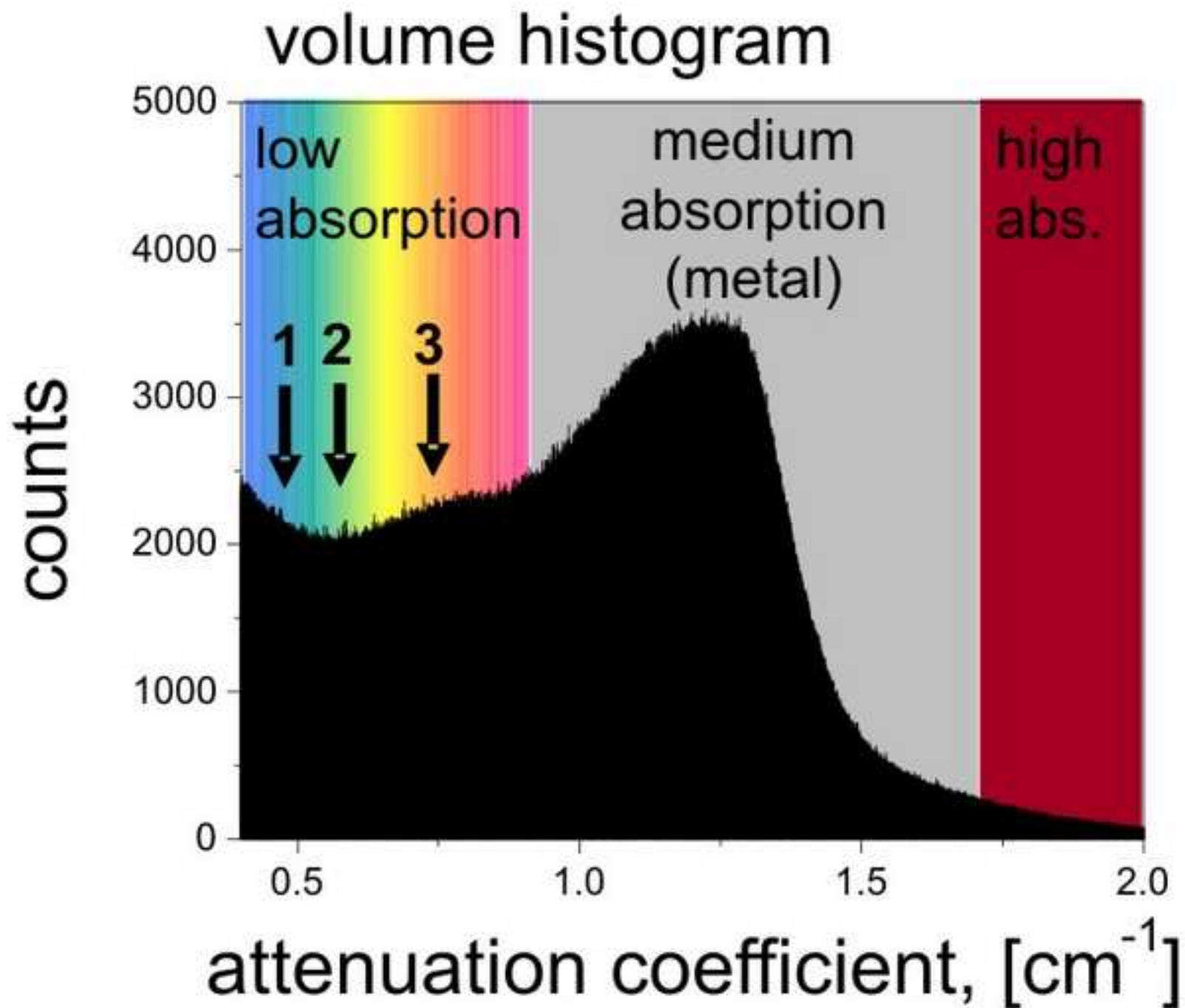


1 cm

Figure(s)
[Click here to download high resolution image](#)

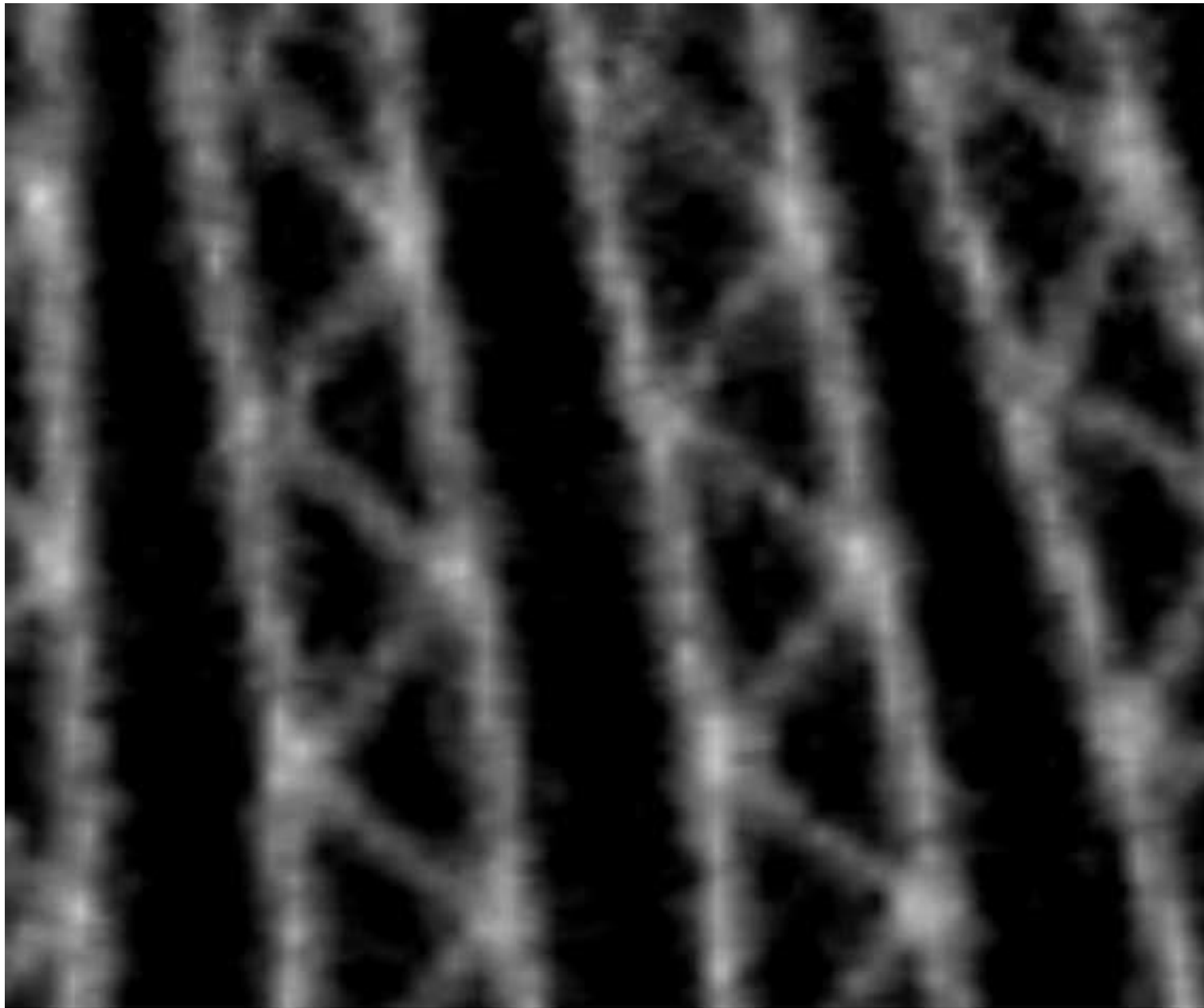







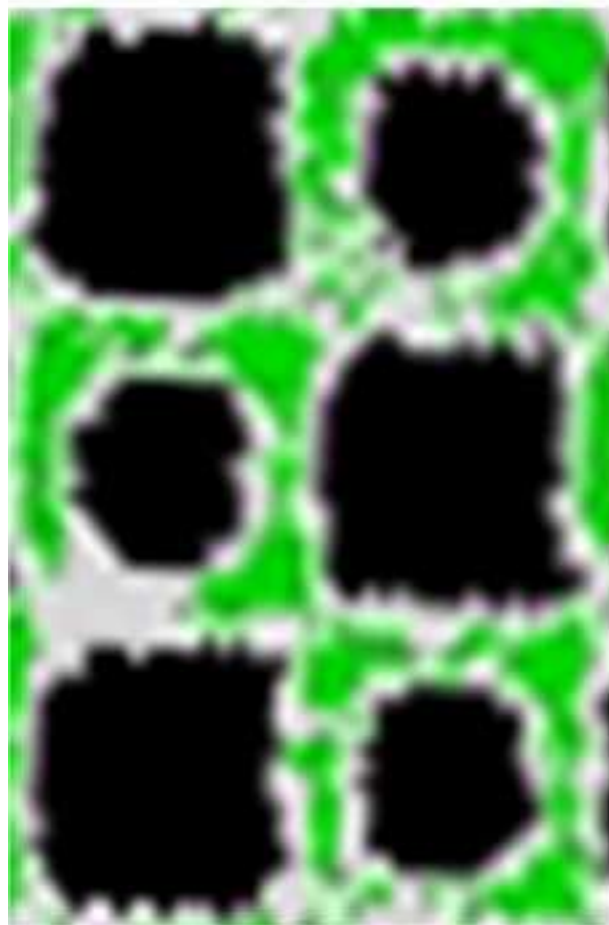
Figure(s)

[Click here to download high resolution image](#)

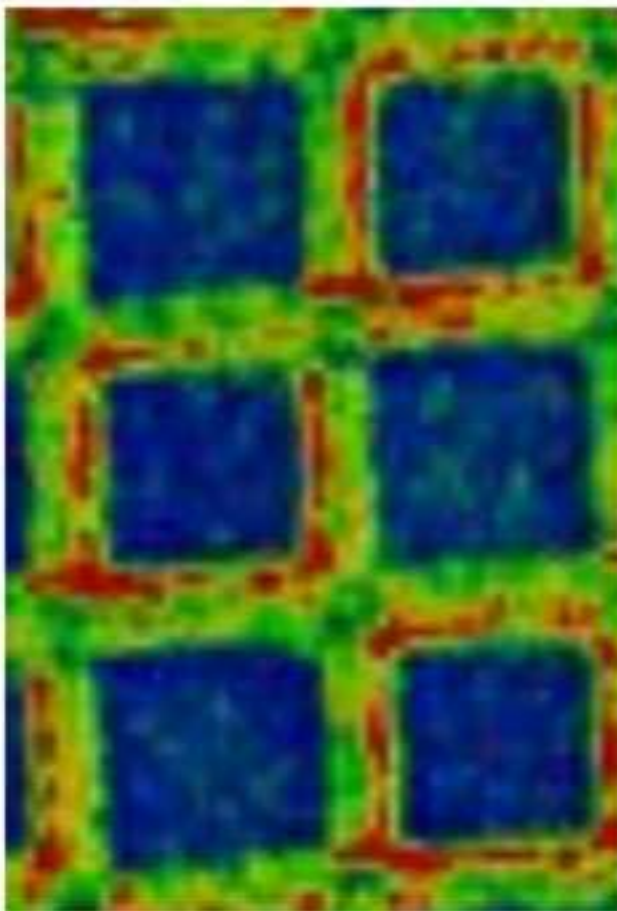



1 mm

(a)



(b)



(c)

